SSIM 2025 - JJ Potter & J Wesseloo (eds)

doi:10.36487/ACG_repo/2535_39

De-risking a Pilbara iron ore pit slope design through a stochastic structural stability assessment

Steve Rogers [a,*], Ciara Byrne [b], Yaniv Fogel [a], Pedro Ojeda [a], Verne Pere [c], Collin Correia [c]

[a] *WSP, Canada*

[b] *WSP, UK*

[c] *Fortescue, Australia*

Abstract

Assessing some of the key risks associated with advancing pit slope design can be challenging during early mine life, with geotechnical data primarily focused on project development and a relatively immature structural model. With data uncertainty being relatively high at this stage, it is not always easy to identify what the critical controls are on inter-ramp and overall wall-scale stability. An assessment on a double pit design, separated by a central pillar – within the Pilbara region of Western Australia – utilised a discrete fracture network (DFN) based approach to assess structural stability uncertainties. The DFN included a regional scale structural model, as deterministic larger scale major brittle structures, along with stochastically generated intermediate-scale -bedding related structures, joints, and fault structures. Material and fault geometry properties were defined for litho-domains using available geotechnical logging and pit mapping data from the first few benches of the excavation. The combination of deterministic and stochastic structures was then used to identify the potential formation of rock wedges in the wall using the developed DFN model. A large number of DFN realisations were run, with each generating potentially hundreds of thousands of blocks. The stability of each block was evaluated, considering discontinuity strengths, rock mass strengths, and pore pressure. This stochastic structural approach allows the estimation of probability of failure (POF) for each design and the development of heat maps, highlighting areas of potential multi-bench instability. Structurally controlled instabilities were seen to be strongly correlated to the presence of regional fault structures and to achieving dewatering targets. Sensitivities showed that should these faults be stronger than modelled in the design, then both the scale and frequency of potentially unstable blocks are reduced. The results of this study helped guide future data acquisition needs, slope monitoring targets, and improved confidence that structurally controlled mechanisms are well understood and managed in the design.

Keywords: *DFN, limit equilibrium, structural stability assessment, probability of failure, risk assessment*

1 Introduction

At early mine life, assessing some of the key geotechnical risks associated with a pit slope design can be challenging. At this early time, the available data typically consists of project development geotechnical data from borehole drilling, and a relatively immature structural model. With data uncertainty being relatively high at this stage, it is not always easy to identify what the critical controls are on inter-ramp and overall wall-scale stability. In a strong rock mass, key slope scale risks are typically associated with the formation of large kinematically unstable wedges and non-daylighting wedges, created from the intersection of intermediate and large structures. As a first order test, the key faults from the structural model can be tested to identify potential wedges. However, as acknowledged above, the structural model at this early stage of development, with limited exposure, remains somewhat exploration focused rather than developed for operational and geotechnical purposes. Thus, the fault geometries will be highly interpretative, often poorly

* Corresponding author. Email address: steve.rogers2@wsp.com

constrained with a relatively high degree of uncertainty with respect to their location, geometry, interactions and strength properties, all of which may result in no wedge formation. Both operational experience and modelling show that it isn't just the major wireframed structures that cause multi-bench scale kinematic failures. Rather it is often their interaction with intermediate-scale structures or combinations of intermediate structures that result in the formation of critical wedges, daylighting or non-daylighting. As such, addressing the critical risk of large kinematic instabilities using a structural model that was not developed for geotechnical applications, may only represent a minor mitigation of risk. Another challenge that is often faced is that early works exposure of the rock mass may not be representative of conditions in the deeper excavation. This is a common consideration in the Pilbara region of Western Australia, where a deep oxidation zone of the order of 100 m deep or greater, covers the region. Thus, no fresh rock mass may be seen to help guide and constrain the structural model until 5–6 benches have been excavated.

To address these challenges, stochastic structural analysis can be used through discrete fracture network (DFN) analysis and modelling. The DFN approach allows the assessment of structural stability for both deterministic wireframed structures as well as stochastic intermediate-scale structures, coupled with variable rock mass strengths and pore pressure conditions. This allows some of these critical uncertainties to be addressed, the probability of failure (POF) to be computed, and key controls on stability to be determined.

This paper describes the application of the DFN approach to a structural stability assessment of an open pit being developed within the eastern Pilbara area. It describes the workflow applied and the results generated as well as addressing some limitations of the approach.

2 Discrete fracture network overview

DFN models are synthetic realisations of the fracture network, that can be used to identify three-dimensional (3D) rock wedges of various scales and evaluate their stability. For clarity, we largely refer to wedges as blocks within this paper as their geometry can be complex; being defined by more than two structures. The 3 key inputs required for DFN model construction are fracture orientation, intensity, and size. DFN methods are not limited to a specific number of fracture sets, allowing more complex structural patterns to be evaluated, along with multiple failure mechanisms. Stability analyses are performed on 3D blocks of varying geometries and sizes identified for each realisation of the DFN, which allows a more robust assessment of the probability of unstable block formation and expected failure mass based on actual field observations.

For this study, wall-scale stability analysis was carried out using DFN models coupled with a custom stress-based 3D limit equilibrium (LE) tool for a future pit design to identify composite (i.e. involving failure through structure or a combination of structure and rock mass) and property (i.e. rock mass strength) controls on slope stability. The aim of the wall-scale model is to assess block formation and the potential for inter-ramp (IR) instability for all domains simultaneously. The wall-scale model combines the intermediate-scale fabric of the fracture network with the deterministic structures (e.g. regional faults), the pit shell, and the rock mass properties of each domain. The FracMan software (WSP 2025) identifies blocks behind the modelled slope and calculates a Factor of Safety (FoS) to categorise the stability of each block. WSP has enhanced the capabilities of the DFN-based analysis by developing the LE code known as 3DPOF.

In addition to the structural component in the DFN model, 3DPOF considers rock mass strength and pore pressure in the stability assessment. Thus, 3DPOF allows structural complexity, varying rock mass strength, and the impact of water pressure to be addressed at IR or wall-scale; at relatively limited computational cost. This method performs probabilistic analysis whilst assessing the sensitivity of the response of the slope to a variety of rock mass strengths and pore pressures.

At the time of the study, the objective of the DFN modelling was to represent the fault system that has been interpreted for the project, which is currently largely unseen apart from borehole intersections, and to evaluate the impact of those faults on stability.

The 3 key inputs required for the stochastic DFN model generation, as introduced above, are:

- structural orientation distribution

- fault intensity and the spatial distribution of the faults
- fault size distribution.

Fault orientations were determined from a combination of televiewer (TV) and photogrammetry data. Fracture intensity was estimated from TV data and the frequency of faults observed. Fracture size distribution was estimated using photogrammetry mapping and large-scale regional fault models from the main pit and nearby mapping. The geometric inputs for the DFN models are outlined in Section 4.

3 Project overview

The open pit that was modelled for this study, and described within this paper, is in the eastern Pilbara area of Western Australia. The orebody is hosted within the deep marine Pincunah Banded Iron Member within the Cardinal Formation of the Soanesville Group. A stratigraphic column and a lithostratigraphic column are shown in Figure 1 for reference. The unconfined compressive strength of the intact rock is typically greater than 200 MPa with planned vertical depths of the pits to approximately 600 m deep. Typical geological strength index

(Hoek et al. 2013) value of the fresh Pincunah Formation is approximately 70, with the oxide around 50. Mining progress at the time of the study was approximately 4–5 benches and was approaching the base of the oxide zone (comprising ferruginous weathered Banded Iron Formation (BIF), detritus, and silcrete) which is 40–60 m thickness (but variable).

The structural setting of the site includes shallow dipping structures, near vertical faulting, steeply dipping bedding, and small-scale folding and faulting. The structural model confidence was assessed as ‘low’ at the time of this study, as it was primarily developed as an exploration scale model, rather than a pit scale structural model with operational geotechnical applications. Data was available from interpreted televiewer surveys conducted in geotechnical drillholes, as well as from photogrammetry mapping performed on the excavated benches. Both a geological model and fault wireframe model were available. Potential failures are anticipated to be predominantly structurally controlled due to the high strength of intact rock with some impact of the rock mass. It should be stressed that the project described here is not representative of many more typical Pilbara banded iron ore formation deposits, within the Brockman or Marra Mamba Iron Formations, where stability is usually controlled by shale bands (bedding) within the BIF units.

4 Discrete fracture network model building and analysis

DFN models aim to explicitly represent the rock mass fabric through the generation of discrete fracture objects. In the case of this project, the objective was to primarily describe the geometry of the fault system and intermediate-scale brittle structures. This comprises of both the regional interpreted structures (wireframes), and the intermediate-scale faults, joints, and bedding related features which were stochastically generated. At this relatively early stage of project construction, the proportion of interpreted wireframed structures to inferred stochastic structures was relatively low. However, as mining continues, exposing more rock mass and as the structural geological model becomes more operationally rather than exploration focused, the proportion of wireframed structures to stochastic structures will increase.

The methodology for defining the key properties of orientation, fault intensity, and fault size distributions are described below as well as how the DFN model is built.

4.1 Fault orientation definition

Structural orientation data were available from televiewer logging of the boreholes (approximately 16 km of drilling) and photogrammetric mapping data of shallow benches within the oxide zone. The orientation analysis included investigating variability of fault/shear orientation by lithology, elevation, fault block, and fault proximity. The dominant control on orientation populations was interpreted to be the lithological units, which are referred to as ‘litho-domains’, and are discussed further in Section 4.4.

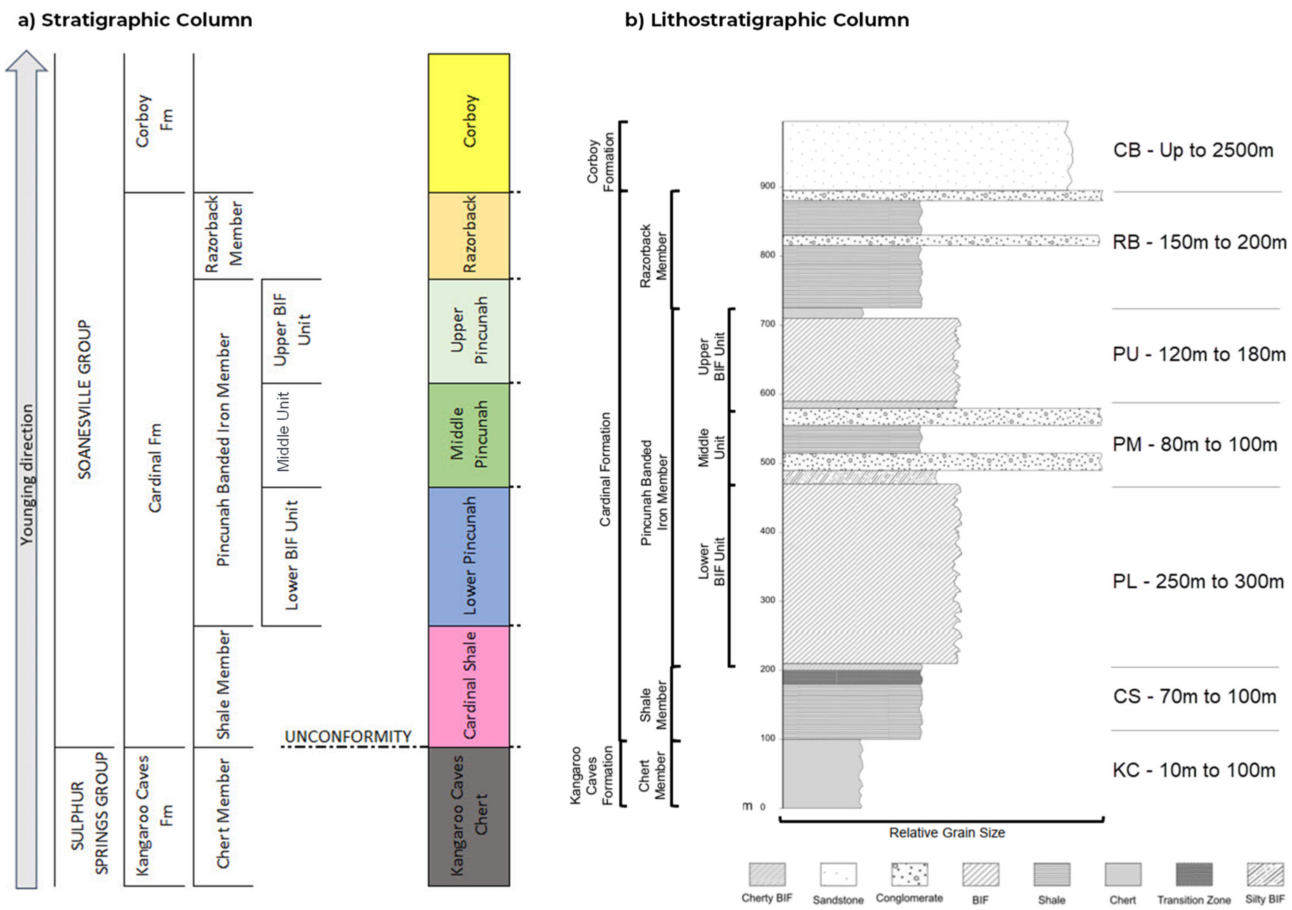

Figure 1 (a) Stratigraphic column; (b) Lithostratigraphic column for the project

Orientation distributions were defined for the 5 identified sets of faults seen in Figure 2a using either a Fisher distribution (i.e. defined by a mean orientation and dispersion factor) or using the statistical technique of bootstrapping. The bootstrapping process randomly samples from the raw orientation dataset, whilst adding a specific degree of dispersion to each pole in order to generate a simulated set of orientations, that are similar but not identical to the actual measured data. This orientation description is ideal for modelling fracture populations that are more dispersed, or with only weak clustering of poles. Stereographic projections for two litho-domains are shown in Figure 2 and an orientation summary is provided below.

- Set 1 is observed in both the borehole and mapping data as a strong concentration. The orientation distribution of this set was defined using Fisher properties. Set 1 represents the bedding orientation and captures larger weaker bedding parallel structures. This bedding does vary on a small-scale, but for the DFN model it was larger bedding parallel breaks that were being captured.
- Sets 2 and 3 are observed in both the borehole and mapping data as relatively weak concentrations without clear Fisher properties. To address this, the raw orientation data was split into two subsets; dipping to the northeast and to the southwest, which were then reproduced using bootstrapping.
- Set 4 is a dispersed set that comprise of a low proportion of the total number of poles. This set has not been generated in the DFN model.
- Set 5 mean orientation was defined using TV data, defined using Fisher distribution properties. Note Set 5 structures were almost exclusively seen in the oxide zone, Figure 2b.

Sets 2, 3, 4 and 5, represent the main trends of open faults seen from the data.

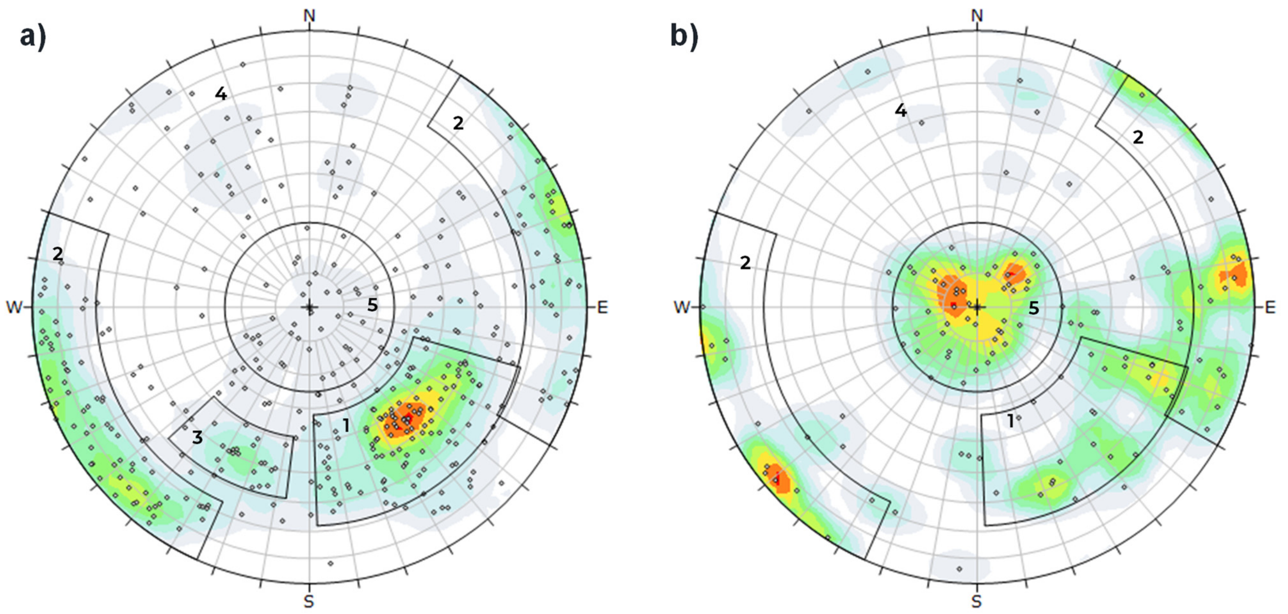

Figure 2 Televiewer orientation data for two litho-domains. (a) One comprised of fresh formations; (b) Near surface oxide-transition zone

To honour the fracture architecture that is observed in the data within the DFN model, the relationship between dominant structures in the deeper fresh units and in the shallower oxide units needs to be considered. The structures that are present in the fresh units persist pervasively through the entire rock mass sequence up into the oxide zone, whilst the flat-lying structures (Set 5) are predominantly found in the oxide zone. The conceptual model (illustrated in Figure 3) captures this:

- The 'fresh' orientation distribution is generated within the entire fresh and oxide sequence, which includes a low intensity of flat structures.
- The 'oxide' orientation distribution only generates the flat structures that are dominant in the oxide stereonet. The other orientations are considered to be representative of structures that are associated with the fresh units.

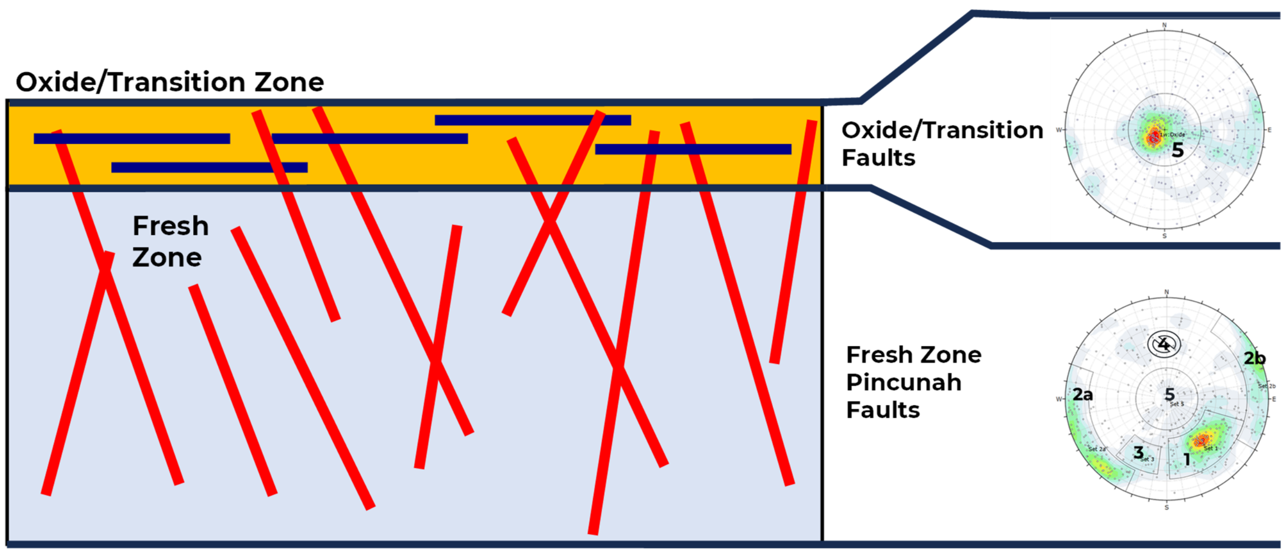

Figure 3 Conceptual orientation model

4.2 Fault intensity properties

A key input to DFN analysis is the calculation of fault intensity, which are discussed using the Pij classification system (Dershowitz & Herda 1992). Conventionally recorded fracture frequency measurements are expressed as fractures per metre (P10 using the Pij notation). Volumetric fracture intensity (P32), defined as surface area of fractures per unit volume, is the preferred measure of fracture intensity in DFN modelling and is typically calculated from borehole derived P10, using the approach proposed by Chilès et al. (2008). P10 fault intensity data were available from boreholes drilled across the two pits, summarised in Figure 4. P10–P32 properties were calculated over the full interval length of the geological units in each borehole. However, Figure 4 shows P32 displayed over smaller composited intervals to illustrate how the faults are distributed with the rock mass. Note the current limited coverage of the central pillar rock mass and the final pit walls.

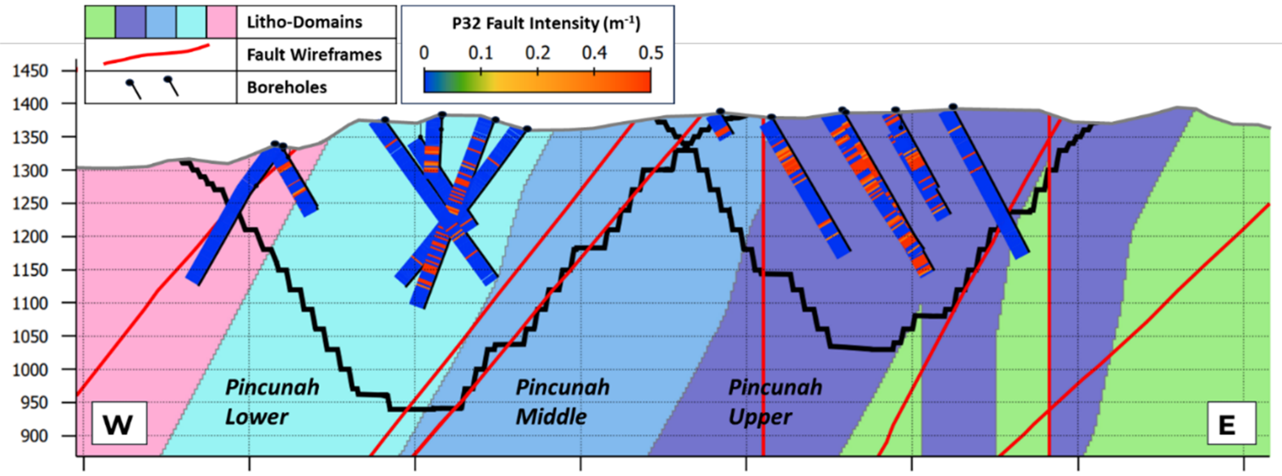

Figure 4 Section across the pit showing the limited data outside the Pincunah Lower and Pincunah Upper

Representative fault intensity values for the fresh and oxide zones are summarised in Table 1.

Table 1 Typical fault frequency and intensity values for fresh and oxide zones

Domain	P10 (m^{-1})	P32 (m^{-1})
Typical oxide formations	0.05	0.06
Typical fresh formations	0.08	0.10

It is noted that the average fault intensity is seen to be higher in the fresh formations, relative to the oxide zone. This is primarily because of the averaging of intensities across different formations. In general, the fresh and oxide zones have broadly similar fault intensities, but within individual formations they can be quite varied. In the future, with more drilling, this difference will be smoothed out.

4.3 Fault size definition

Defining the size distribution of faults at an early stage of mining, when there is limited exposure available to map structures, remains challenging. The use of power law analysis is typically employed to infer the fault size distribution from measurements at different scales. The power law analysis technique (e.g. Rogers et al. 2016) reflects the common observation that many geological structures show scale invariant properties over large-scale ranges. Using this method, data measured over several orders of magnitude can be plotted together and, where appropriate, a single common power law trend identified for the size of structures spanning a wide range of length scales.

In the case of this project, data were available from the regional structural model, fault modelling nearby, and photogrammetry analysis in the initial benches of the pit. Based on the power law plot, the straight-line gradient of −1.68 has been used to stochastically assign persistence to the generated fault structures. The power law plot considered for this study is presented in Figure 5.

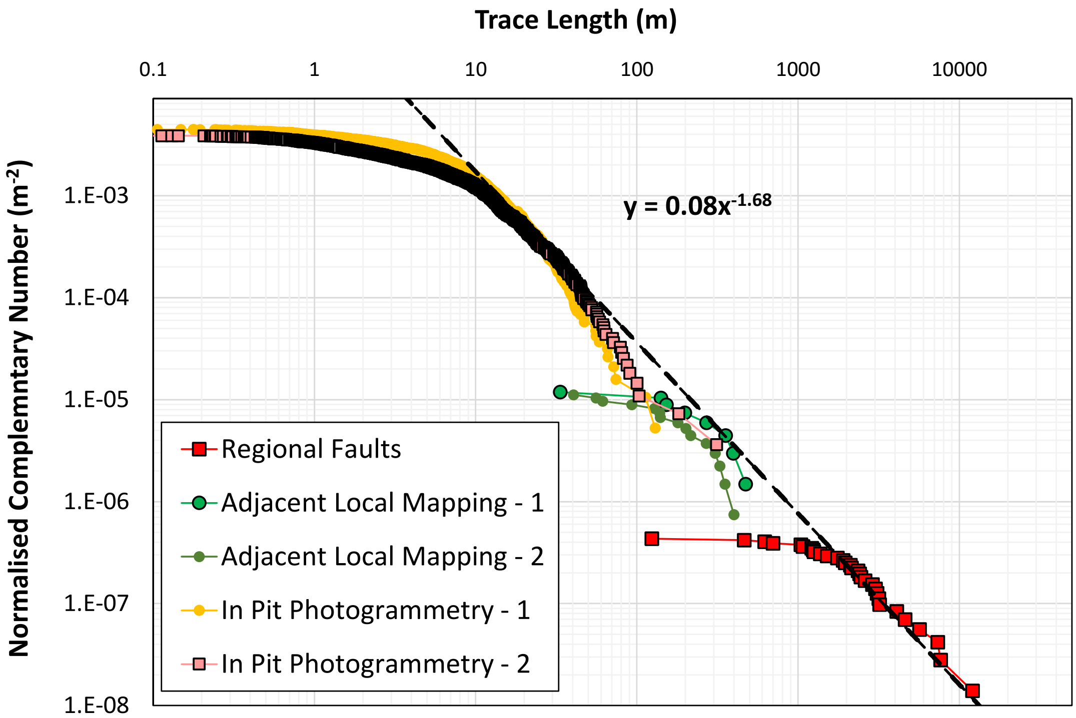

Figure 5 Power law analysis of fault structure length

4.4 Model build

The DFN model represents a combination of the regional wireframed faults and the intermediate-scale stochastic faults. The stochastic faults were generated within a geocellular grid that encompassed the extents of the pit design and was populated with attributes that identify the location of the various geological units, and the oxidisation zone. The lithological units (i.e. litho-domains), which were observed to be the key control on the structural variability in the fracture network, were used as the primary generation partitions for the different fracture sets (Figure 6a).

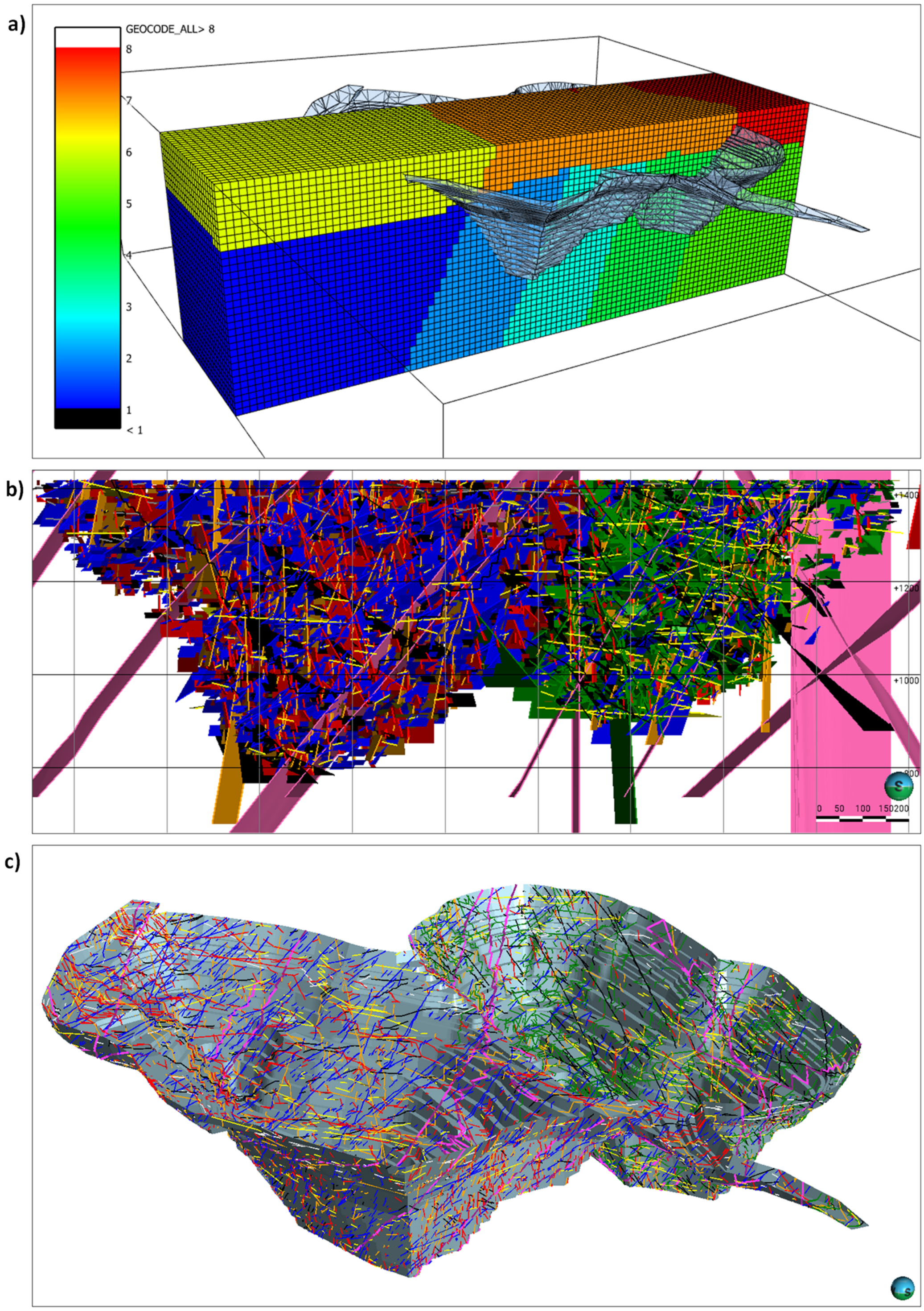

Figure 6 (a) Part of the geocellular model with litho-domains displayed, which were used to generate the discrete fracture network (DFN) model; (b) East–west section through the pit and the DFN model; (c) Oblique view of pit with the DFN model intersections mapped onto the pit shell

The stochastic faults were generated within 150 m of the pit shell (3D distance). An external view of one realisation of the DFN model in shown in Figure 6b and an internal view, showing the intersection of the simulated faults on the pit shell, Figure 6c. Note the relatively sparse nature of the simulated fault network, which is consistent with field observations. The regional wireframed faults within the DFN model are comprised of 72 wireframes.

5 Stability assessment

5.1 DFN-3DPOF approach overview

Having developed the DFN description of the project fault system, each DFN model realisation is searched to identify 3D blocks forming behind the slope. These blocks are assessed for simple kinematic stability using a conventional LE solution. Smaller blocks (up to two benches) may be unstable, whilst the larger multi-bench scale blocks are typically locked in and kinematically stable because the block is sitting behind or beside a buttress of rock mass that potentially prevents sliding.

The FracMan® generated blocks are extracted and have their stability assessed using the 3DPOF code. The 3DPOF analysis considers the stability of every block using a custom slip surface approach described in Lawrence et al. (2020). The approach considers the rock mass strength, joint strength, and pore pressure conditions. It is a computationally rapid LE solution, allowing a wide range of scenarios and sensitivities to be evaluated at very limited computational cost. The approach is described more fully in Valerio et al. 2021 and Rogers et al. 2023. The rock blocks that form can be any size, but this assessment was focused on blocks that were more than the scale of a single bench. To focus the analysis on this block scale, only blocks with a volume greater than 7.5 × 7.5 × 7.5 m (421.9 m^3) were processed. The 3DPOF analysis requires the definition of generalised Hoek–Brown (Hoek et al. 2002) strength properties for the rock mass strength and Mohr–Coulomb properties for the fault strengths. Pore pressure is defined using Ru (Wylie 2003).

The aim of the wall-scale model is to assess block formation and potential instability for all geotechnical domains and sectors simultaneously. The wall-scale model combines the stochastic fault fabric of the fracture network with the deterministic 3D fault wireframe structures in an in situ model that includes the pit shell, lithology (i.e. litho-domains), and 3D rock mass properties.

The 3DPOF approach produces two different results as follows:

- estimates of the derived POF results for each litho-domain, based upon a failure volume (tonnage) metric
- estimates of where blocks may form and where these may be unstable within the pit shell.

The use of a POF proxy, which is referred to as cell failure percentage (CF%), was used to visualise these results as density heatmaps.

Assessing the stability of blocks forming in the central pillar between the east and west pits requires a slightly different approach. Blocks forming within the pillar have the potential of sliding in either direction (eastwards or westwards). Blocks that form within the pillar are evaluated based upon the likely direction of their valid failure path. Blocks that have valid paths in both directions are evaluated based on the lower FoS assigned for each direction, Figure 7.

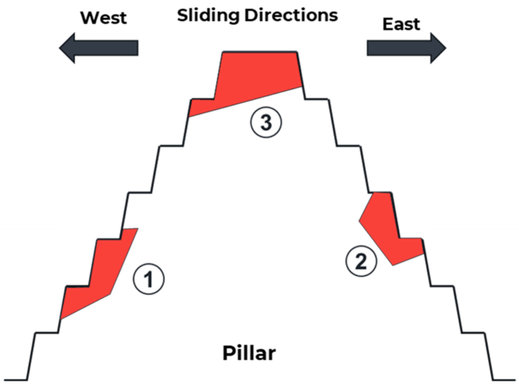

Block	Sliding Direction	
	West	East
1	Valid	Not Valid
2	Not Valid	Valid
3	Valid (FOS <1)	Valid (FOS >1)

Figure 7 The logic for evaluating stability of multi-bench scale blocks that were identified within the central pillar

5.2 DFN-3DPOF results

The significance of wireframed regional faults on the formation of large blocks and their potential instability is well known. At this early stage of pit development, the geometry, characteristics, and strength properties of these larger structures represent relatively high levels of uncertainty. To help address this, two separate models were analysed to investigate the stability of the pit slopes: a model with both stochastic structures and wireframed regional faults and a second model with just stochastic structures (i.e. no regional fault wireframes). This allows the large-scale faults to be considered with regard to the impact they have on stability.

To compile the results of 100 realisations of the analysis, heatmaps of two properties were generated. The first property is called the probability of block occurrence (POBO) and is computed by counting – for every cell on a surface – the number of realisations where blocks formed, divided by the total number of realisations (typically 100). This gives a measure of where blocks are most likely to form. The second property is called CF% and represents, the number of realisations with unstable blocks/wedges, divided by the total number of realisations (typically 100), for every cell on the pit shell surface. This property represents a local POF metric. An example of the derivation of a CF% heat map is shown, Figure 8.

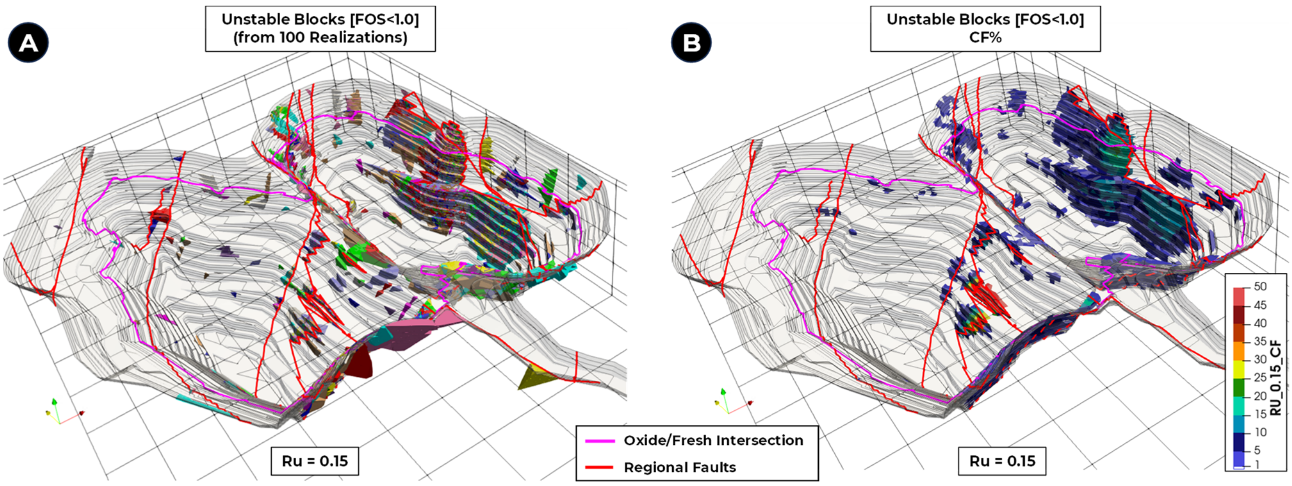

Figure 8 (a) Oblique view of all unstable blocks/wedges formed from 100 DFN realisations (blocks coloured by realisation number); (b) Oblique view of a heat map showing the cell failure percentage (CF%)

In addition to the structural model uncertainty, pore pressure conditions are often poorly defined at early mine life. To address this, base case pore pressure conditions use an Ru = 0.15. This is considered representative of a pit with moderate pore pressure, but reasonable groundwater management and/or effective drainage. However, pore pressure sensitivity simulations were also carried out (shown later) to address the role that water can play in the stability of the slope. POBO heat maps (Figure 9) and CF% heat maps (Figure 10) are presented for the scenario with both stochastic and regional faults, and the scenario with just stochastic faults. POBO indicates zones of increased block formation, Figure 9.

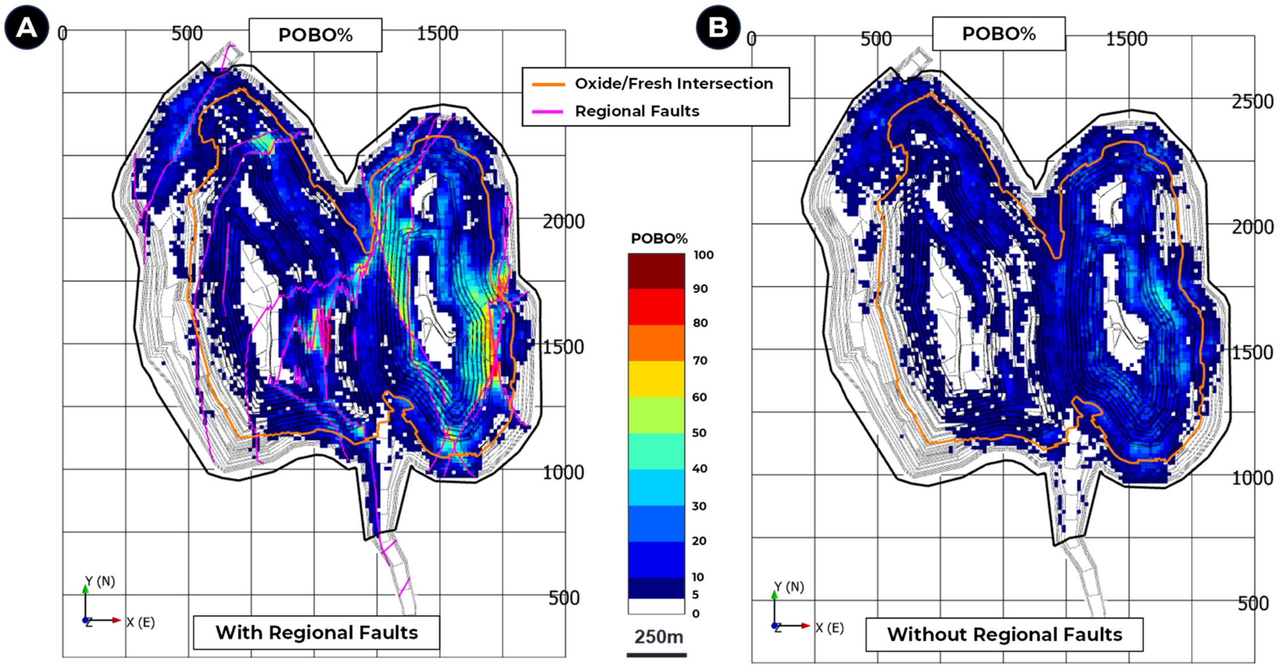

Figure 9 DFN-3DPOF POBO results. (a) With regional faults; (b) Without regional faults

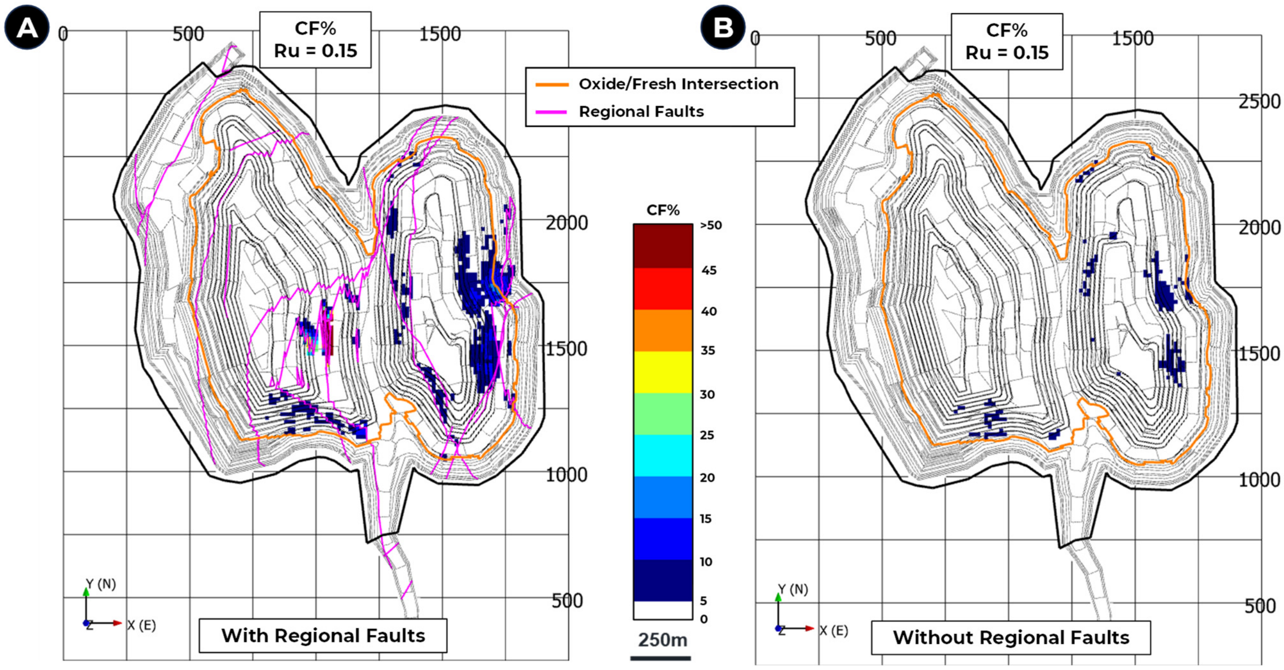

Figure 10 DFN-3DPOF CF% results, at Ru = 0.15, with base case strength. (a) With regional faults; (b) Without regional faults

In the model with regional faults included (Figure 9a), areas of elevated POBO (≥30%) are observed near intersections of regional structures. This suggests that the regional fault structures play a significant role in the formation of larger blocks and indicates that the complex kinematic blocks are formed by a combination of both regional faults and the stochastic structural fabric. Areas with a POBO greater than 80% are noted on the west side of the central pillar, and on the east wall of the eastern pit. Note, that when regional faults are not included in the model, areas of elevated POBO (≥30%) are significantly reduced, again suggesting that the formation of complex kinematic blocks is a combination of the stochastic structural fabric and local slope design.

Figure 10 presents a plan view with the CF% results for the base case strength models with regional faults (Figure 10a) and without regional faults (Figure 10b); for a base case pore pressure of Ru 0.15. Whilst not a true measure of POF at the slope scale, CF% represents a local POF measurement and can be used to identify potentially unstable areas in the pits.

When regional fault wireframes are included in the model, the results show that areas with a CF% ≥ 5% are generally located along those faults, on the south and southeast slopes of the western pit, and mostly on the east slopes of the eastern pit. Areas of CF% greater than 10% are noted near the intersection of regional faults, specifically the west side of the pillar, and on the east wall of the eastern pit. In contrast, when regional faults are not included in the model, it can be observed that areas with CF% ≥ 5% have decreased significantly in both size and intensity, with the model showing no areas with CF% greater than 10%. CF% between 5% and 10% are mostly observed on the south slopes of the western pit, and the east and west slopes of the eastern pit.

The base case CF% results shown above, used the base case Ru value of 0.15 which is considered to represent a moderate pore pressure condition. To investigate the impact of more conservative (i.e. higher) pore pressure conditions, sensitivity simulations were run for the scenario with regional faults and base case strength conditions. Figure 11 shows CF% results for Ru values of 0.15, 0.3, and 0.4.

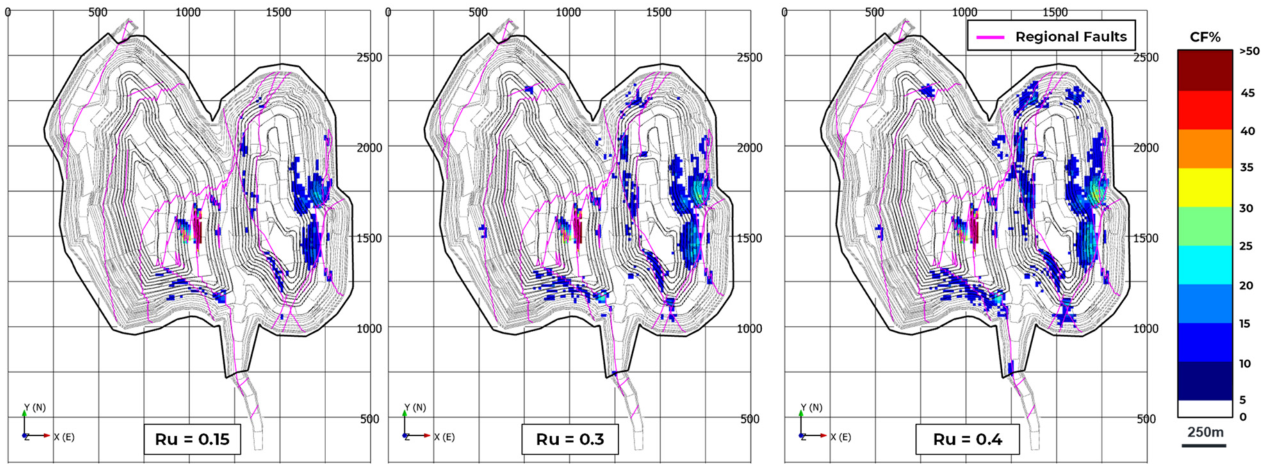

Figure 11 DFN-3DPOF CF% results with regional faults included and base case strengths, at three different Ru values

Pore pressure conditions are observed to have a major impact on stability in the model. As pore pressure increases (Ru = 0.3 and 0.4), areas of elevated CF% values start to develop along the intersections of regional faults on the east and west walls of the eastern pit. Areas of CF% ≥ 5% also start to develop on the south slopes of the western pit. Areas of elevated CF% increase in size and intensity at higher pore pressures (Ru = 0.3 and 0.4). Additional 'hot spots' of instability begin to develop on the north slopes of the eastern pit and the north slopes of the western pit.

In the same way pore pressure sensitivities can be used to identify critical pore pressure levels, a range of different Hoek–Brown strength properties and Mohr–Coulomb fault strengths can also be tested to determine any stability controlling strength properties.

POF results can also be computed for each litho-domain based on the ratio of the volume of unstable blocks to total blocks formed within a domain. Example results are shown for various POF results as a function of Ru, Figure 12.

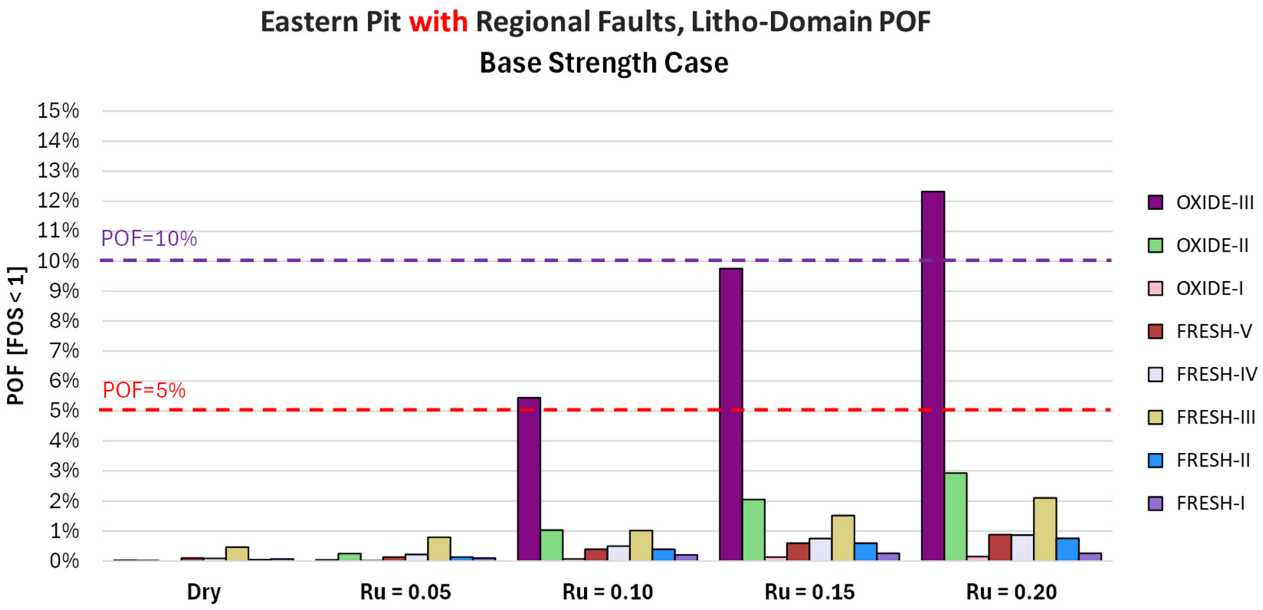

Figure 12 POF by litho-domain for the model with base case strength and regional faults included

The results show that at relatively dry conditions (i.e. Ru = 0.0 and 0.05), the POF for all litho-domains was below the 5% design threshold for high risk, Read & Stacey 2009. As Ru increases, it can be noted that the Oxide-III domain exhibits a steep increase in POF values. For the model that includes regional faults, Ru values greater than 0.10 result in the Oxide-III domain slightly exceeding the 5% POF design threshold. These higher POF values are interpreted to be related to the presence of multiple closely spaced regional fault wireframes. The interaction of these wireframe faults with the stochastic fracture network results in the formation of infrequent multi-bench scale blocks, which are unstable under elevated pore pressure conditions. Although the number of unstable blocks generated in this litho-domain is small, the blocks that form can have significant volumes. For that reason, each calculated unstable block results in a steep increase in the POF value.

6 Summary

This analysis shows the critical role that the larger structures play in the formation of potential instabilities in both of the open pits. It is both the interaction of major regional structures (wireframes) and the interaction of regional structures and stochastically modelled intermediate-scale structures, that define the majority of potential fully formed blocks; many of which represent unstable volumes on the multi-bench scale, particularly under elevated pore pressure conditions. Comparing the results for the cases with and without the major faults, where potential instabilities are significantly lower, shows how critical the larger structures are to the formation of blocks. This clearly identifies the need for advancing the site structural model from the initial coarser exploration focused model with relatively high geometric uncertainty, to a more operationally focused geotechnical structural model where fault locations, geometries and strengths are better constrained. Obviously, this will happen as the pit advances and more wall is exposed, particularly in the fresh zones.

Despite the relatively low fault intensity, the ability of the fault network to form potentially problematic wedges (either daylighting or non-daylighting) is relatively high. This is to some degree due to the simulated lengths of structures which follow a power law trend. Establishing greater confidence in both the distribution of lengths and the range of sizes observed would reduce this uncertainty within the model inputs.

The modelled impact of increasing pore pressure shows the impact of poor water management, in particular an increase in failure tonnage and CF%. The results show that, if pore pressures can be reduced and managed at lower levels, POF values are seen to be reduced. Although the issue of pore pressure is important, understanding the nature of pore pressure distribution is not straightforward. In a very tight rock mass with little primary porosity, it will generally be a sparse network of structures that primarily carry any groundwater. This will have implications for future drainage activities and their effectiveness, as well as how the pore pressure distributes itself within the rock mass.

This project set out to help de-risk an early mine life open pit project from the perspective of structurally controlled instability. The DFN part of the analysis helped capture structural patterns and allowed multi-bench scale blocks to be identified, whilst the 3DPOF LE analysis allowed the stability of these blocks to be evaluated and to constrain critical controls on potential instability. As the pits deepen and more data are acquired and the structural model develops, the approach can be used both as a risk assessment tool looking ahead over potential instabilities that may be encountered over the next period, as well as for slope design.

Acknowledgement

We would like to acknowledge Fortescue for permission to publish this paper and their support throughout the project.

References

Chilès, JP, Wackernagel, H, Beucher, H, Lantuéjoul, C & Elion, P 2008, 'Estimating fracture density from a linear or areal survey', in JM Ortiz & X Emery (eds), *Geostats 2008: Proceedings of the Eighth International Geostatistics Congress*, Gecamin, Santiago, pp. 535–544.

Dershowitz, WS & Herda, HH 1992, 'Interpretation of fracture spacing and intensity', in JR Tillerson & WR Wawersik (eds), *Proceedings of the 33rd US Rock Mechanics Symposium*, AA Balkema, Rotterdam.

Hoek, E, Carranza-Torres, CT & Corkum, B 2002, 'Hoek-Brown failure criterion – 2002 edition', *Proceedings of the Fifth North American Rock Mechanics Symposium,* University of Toronto Press, Toronto, vol. 1, pp. 267–273.

Hoek, E, Carter, TG & Diederichs, MS 2013, 'Quantification of the geological strength index chart', in LJ Pyrak-Nolte, A Chan, W Dershowitz, J Morris, J Rostami (eds) *Proceedings of the 47th Rock Mechanics/Geomechanics Symposium*, American Rock Mechanics Association, Eaton, pp. 1757–1764.

Lawrence, KP, Nelson, MD, Yetisir, M & Matlashewski, P 2020, 'Kinematic assessment of composite failure mechanisms in pit slopes — a novel slip surface identification algorithm for DFN models', *Proceedings of the 54th US Rock Mechanics/Geomechanics Symposium*, American Rock Mechanics Association, Eaton.

Read, J & Stacey, P 2009, *Guidelines for Open Pit Slope Design*, CSIRO Publishing, Collingwood.

Rogers, SF, Elmo, D, Webb, G & Guajardo Moreno, C 2016, 'DFN modelling of major structural instabilities in a large open pit for end-of-life planning purposes', *Proceedings of the 50th US Rock Mechanics/Geomechanics Symposium*, American Rock Mechanics Association, Eaton.

Rogers, S, Valerio, M, Fogel, Y, Byrne, C & Ojeda, P 2023, 'Evaluation of inter-ramp scale non-daylighting wedges using a discrete fracture network-based method', in PM Dight (ed.), *SSIM 2023: Third International Slope Stability in Mining Conference*, Australian Centre for Geomechanics, Perth, pp. 951–964, https://doi.org/10.36487/ACG_repo/2335_65

Valerio, M, Rogers, S, Lawrence, KP, Moffitt, KM, Rysdahl, B & Gaida, M 2020, 'Discrete fracture network based approaches to assessing inter-ramp design', in PM Dight (ed.), *Slope Stability 2020: Proceedings of the 2020 International Symposium on Slope Stability in Open Pit Mining and Civil Engineering*, Australian Centre for Geomechanics, Perth, pp. 1017–1030, https://doi.org/10.36487/ACG_repo/2025_67

WSP 2025, *FracMan Interactive Discrete Feature Data Analysis, Geometric Modeling, and Exploration Simulation User Documentation*, version 8.4, WSP, London.

Wyllie, DC 2003, *Foundations on Rock: Engineering Practice*, 2nd edition, CRC Press, New York.